

Incremental Gauss-Newton Descent for Machine Learning

Mikalai Korbit[†]

Mario Zanon[†]

DYSCO (Dynamical Systems, Control, and Optimization)[†]
IMT School for Advanced Studies Lucca, Italy

August 13, 2024

Abstract

Stochastic Gradient Descent (SGD) is a popular technique used to solve problems arising in machine learning. While very effective, SGD also has some weaknesses and various modifications of the basic algorithm have been proposed in order to at least partially tackle them, mostly yielding accelerated versions of SGD. Filling a gap in the literature, we present a modification of the SGD algorithm exploiting approximate second-order information based on the Gauss-Newton approach. The new method, which we call Incremental Gauss-Newton Descent (IGND), has essentially the same computational burden as standard SGD, appears to converge faster on certain classes of problems, and can also be accelerated. The key intuition making it possible to implement IGND efficiently is that, in the incremental case, approximate second-order information can be condensed into a scalar value that acts as a scaling constant of the update. We derive IGND starting from the theory supporting Gauss-Newton methods in a general setting and then explain how IGND can also be interpreted as a well-scaled version of SGD, which makes tuning the algorithm simpler, and provides increased robustness. Finally, we show how IGND can be used in practice by solving supervised learning tasks as well as reinforcement learning problems. The simulations show that IGND can significantly outperform SGD while performing at least as well as SGD in the worst case.

1 Introduction

Many problems in Machine Learning (ML) are formulated as optimization problems that can be solved by gradient-based methods. Stochastic Gradient Descent (SGD) is a first-order stochastic optimization algorithm formally introduced by [35] which has become the backbone optimization algorithm for many machine learning tasks. While being effective and computationally simple, SGD can in some cases converge slowly in the flat regions of the loss function landscape [22]. Many acceleration methods have been proposed to overcome this issue, among others, momentum-based approaches [7, 23, 29, 38], adaptive learning rates [10, 14, 49] or a combination of the two [9, 18, 46]. Recent successes in training very large neural networks can be partially attributed to the advances in such optimization algorithms [42].

Another approach to improve first-order methods consists in (approximately) accounting for second-order information [45], such that the descent direction is calculated by solving the linear system $\mathbf{H}\mathbf{d} = -\mathbf{g}$ where \mathbf{H} is the (approximate) Hessian matrix and \mathbf{g} is the gradient of the loss function. The adaptation of these algorithms to ML problems is challenging due to the high dimensionality of the search space, which makes it hard to compute and store second-order sensitivities as well as to solve the (typically dense) linear system, which scales cubically with the dimension of the search space. This is particularly unfortunate since second-order derivatives carry information about the curvature of the loss

landscape which can yield faster convergence, and these methods are scale-invariant, i.e., more robust and easier to tune.

Motivated by the observations above, the so-called Gauss-Newton (GN) Hessian approximation scheme [30] has been re-examined for application in the stochastic setting. The most promising approaches include the stochastic generalized Gauss-Newton method (SGN) [12] that couples a regularized Levenberg-Marquardt Hessian approximation with a Conjugate Gradient (CG) solver, the Nonlinear Least Squares Rank-L method (NLLSL) [6] and SGN2 [40] that estimate the Jacobian with a rank-L approximation and SARA estimate respectively, as well as SMW-GN [34] that uses the Sherman-Morrison-Woodbury formula to efficiently solve the linear system.

Stochastic optimization approaches can be divided into incremental and batch methods. In this paper, we avoid comparing the two classes and focus on incremental algorithms, while in future work we will extend our method to batch approaches. We propose an incremental update which is as cheap to compute as an SGD update, while at the same time yielding a Gauss-Newton update, i.e., approximately accounting for second-order information. Although the proposed approach requires a relatively small modification to SGD, we argue that the implications are important: the resulting update is effective in practice and, in addition, can be accelerated using the same strategies that accelerate SGD.

Our contributions are as follows.

- We propose the Incremental Gauss-Newton Descent (IGND) algorithm, which relies on the Gauss-Newton Hessian approximation to exploit approximate second-order information and has essentially the same computational cost as SGD.
- We first explain the IGND algorithm in the light of approximate second-order methods for optimization and then show that it can be interpreted as a scale-invariant version of SGD. We finally prove convergence of the IGND algorithm.
- We discuss how IGND can be applied to solving supervised learning and reinforcement learning problems. Through numerical experiments we show that IGND is easier to tune and performs at least as well as SGD, while significantly outperforming it in some cases.

2 Related Work

We provide next a quick overview of the most relevant results available in the literature, divided into three major topics.

Accelerated first-order optimization The de facto default choice of the optimization algorithm for a machine learning task is typically an “accelerated” variation of the Stochastic Gradient Descent (SGD) algorithm [35]. A detailed overview of the acceleration methods can be found in [20] and in survey papers [22, 37], while we mention below some key approaches.

One group of methods is inspired by the Polyak heavy ball (classical) *momentum* [32]. The basic idea is to replace a gradient estimate with an exponential moving average (EWMA) of the current and past gradients. Nesterov Accelerated Gradient (NAG) [29] introduces an additional extrapolation step when computing the EWMA gradient estimate. An adaptation of NAG for training deep neural networks is explored in [38], where the similarities between Polyak’s momentum and NAG are underlined. These approaches require setting a hyperparameter β that regulates the aggressiveness of the averaging. A more recent method called AggMo [23] generalizes the classical momentum by introducing several

velocity vectors with different β parameters. In [7] the authors propose to decay the hyperparameter β over the iterations effectively making the algorithm less sensitive to selecting the best value for β .

Another group of methods (sometimes called *adaptive learning rates* methods) uses diagonal preconditioning of the gradient of the form $\mathbf{D}^{-1}\mathbf{g}$ where \mathbf{D} is a diagonal matrix. Note that preconditioning can be interpreted both as a scaling correction and as an approximation of second-order information. Several practical choices exist for constructing a preconditioner \mathbf{D} . AdaGrad [10] proposes to construct \mathbf{D} as the square root of the sum of the current and past squared gradients. Since AdaGrad’s preconditioner \mathbf{D} grows overly large throughout the iterations, it is beneficial to replace the sum of the squared gradients with the Exponentially Weighted Moving Average (EWMA), which is the main idea in, e.g., RMSProp [14] and AdaDelta [49].

The two groups of methods described above, i.e., momentum methods and adaptive learning rates, can be combined together. The popular optimizer Adam [18] combines the classical momentum with RMSProp diagonal preconditioning. Alternatively, a modified version of the Adam algorithm where the heavy ball momentum is replaced with NAG has been proposed in [9].

Interestingly, we will show that IGND can be accelerated in the same way as the standard SGD, so that the aforementioned acceleration approaches directly apply to the IGND algorithm as well.

Approximate second-order optimization Since computing and storing the exact Hessian matrix is impractical even for moderately sized neural networks, there has been a revived interest in approximate second-order methods. For a comprehensive overview we refer the reader to the survey papers [2, 45]. We focus next on some approaches inspired by the Gauss-Newton Hessian approximation, which are most closely related to IGND.

Stochastic second-order methods that do not rely on computing the full Hessian matrix, also called “hessian free optimization” or HFO, have been proposed by [24]. In [19] the HFO framework is extended with stochastic line search, dynamic regularization and momentum acceleration techniques. The Krylov subspace descent method (KSD) [41] provides an alternative method to calculate an approximation of the Gauss-Newton Hessian. A block-diagonal Gauss-Newton matrix for dense networks is derived in [1] as yet another attempt at constructing the approximate Hessian matrix. The Kronecker Factored Recursive Approximation (KFRA) algorithm proposed in the paper is experimentally shown to converge faster than the accelerated Adam solver. In addition, KFRA requires much less hyper-parameter tuning than the state-of-the-art first-order methods.

The idea of applying the Levenberg-Marquardt (LM) solver to the stochastic setting has been explored in [6, 12, 15, 34, 40]. The stochastic generalized Gauss-Newton method (SGN), introduced in [12], couples a regularized Levenberg-Marquardt Hessian approximation with a Conjugate Gradient (CG) method for approximately solving the linear system. SGN is shown to outperform SGD on several regression and classification tasks. Similarly to block-diagonal Gauss-Newton [1], also SGN requires less hyper-parameter tuning. In [34] the authors propose to use the Sherman-Morrison-Woodbury (SMW) formula as an alternative to the CG solver for solving the linear system. The method is experimentally shown to be competitive with the Hessian-free one proposed in [24] and KFAC [25], with the additional benefit of not requiring any parameter tuning. Another issue with LM-based methods is the calculation of the Jacobian of the residuals. While the predominant approach is to calculate the Jacobian exactly via reverse mode autodiff, alternative methods have been recently proposed. The notable approaches are the Non-linear Least Squares Rank-L (NLLSL) algorithm [6] that builds a rank-L approximation of the Jacobian and SGN2 [40] which proposes the SARAH estimation of the Jacobian.

All these approaches are batch methods, which have the downside of requiring matrix-matrix or matrix-vector multiplications, while SGD and IGND only require operations on vectors. Our algorithm

performs per-sample updates and does not construct the full Hessian matrix, so as to eliminate the need for matrix-matrix and matrix-vector multiplications. Ongoing research is focusing on an extension of IGND to the batch case in a way that mitigates the issue of matrix-matrix and matrix-vector multiplications so as to keep the computational burden low.

Gradient Clipping and Normalized Gradients A well-known issue with training neural networks is related to the so-called *exploding gradients* [26]. A simple solution consists in clipping or normalizing the gradient when it becomes excessively large. A formal analysis of why gradient clipping accelerates learning is provided in [50]. In [33] the authors reformulate the gradient clipping strategy to reflect the clipping techniques used by practitioners and prove the convergence of the Clipped Gradient Descent (CGD). Normalizing the gradient for the least squares problems, which is a well-known technique in signal processing [44], has recently been studied for machine learning applications. In particular, [27] provides the theoretical explanation for the behavior of the Normalized Gradient Descent (NGD) near saddle points while in [28] the authors experimentally show the improved convergence of NGD for various neural network architectures.

The crucial difference between the IGND update and the CGD/NGD step is that, in order to clip or rescale the gradient step, IGND computes the squared norm of the gradient of the function approximator while CGD and NGD are based on the (non-squared) norm of the the gradient of the loss function.

3 Incremental Gauss-Newton Descent

In this section we present our main contribution: the Incremental Gauss-Newton Descent algorithm.

3.1 Problem Formulation

We consider the problem of finding the weights $\mathbf{w} \in \mathbb{R}^m$ of a parametric function $f_{\mathbf{w}} : \mathbb{R}^n \rightarrow \mathbb{R}$, e.g., a neural network, such that it fits some dataset \mathcal{D} consisting of N $\langle y_i, \mathbf{x}_i \rangle$ pairs where y_i is a scalar target and $\mathbf{x}_i \in \mathbb{R}^n$ is a vector of features. We formulate the problem in the standard form

$$\arg \min_{\mathbf{w} \in \mathbb{R}^m} \mathcal{L}(\mathbf{r}_{\mathbf{w}}(\mathbf{y}, \mathbf{f}_{\mathbf{w}}(\mathbf{x}))), \quad (3.1)$$

where \mathcal{L} is the loss function, and

$$\mathbf{y} = [y_1 \quad \dots \quad y_N]^\top, \quad (3.2)$$

$$\mathbf{f}_{\mathbf{w}}(\mathbf{x}) = [f_{\mathbf{w}}^{(1)} \quad \dots \quad f_{\mathbf{w}}^{(N)}]^\top, \quad (3.3)$$

$$\mathbf{r}_{\mathbf{w}}(\mathbf{y}, \mathbf{f}_{\mathbf{w}}(\mathbf{x})) = [r_{\mathbf{w}}^{(1)} \quad \dots \quad r_{\mathbf{w}}^{(N)}]^\top, \quad (3.4)$$

with

$$f_{\mathbf{w}}^{(i)} = f_{\mathbf{w}}(\mathbf{x}_i), \quad r_{\mathbf{w}}^{(i)} = r_{\mathbf{w}}(y_i, f_{\mathbf{w}}(\mathbf{x}_i)). \quad (3.5)$$

We assume all these functions to be twice differentiable with respect to \mathbf{w} . Note that, while this assumption could be relaxed, we stick to it for the sake of simplicity.

Problem (3.1) often arises in machine learning, both in supervised learning and in reinforcement learning (RL). We will focus next on losses defined as least-squares

$$\mathcal{L}(\mathbf{r}_{\mathbf{w}}) := \frac{1}{2} \|\mathbf{r}_{\mathbf{w}}\|^2 = \frac{1}{2} \mathbf{r}_{\mathbf{w}}^\top \mathbf{r}_{\mathbf{w}}, \quad (3.6)$$

where we use $\mathbf{r}_w = \mathbf{r}_w(\mathbf{y}, \mathbf{f}_w(\mathbf{x}))$ and $r_w^{(i)} = y_i - f_w(\mathbf{x}_i)$. Nevertheless, it is possible to extend our approach to cover more generic loss functions, such as, e.g., the negative logarithmic loss function and semi-gradient approaches common in RL.

3.2 Gradient-Based Optimization

Problem (3.1) is typically solved by variations of the gradient descent (GD) method. Although the problem appears to be formulated in a deterministic way, in ML applications it is solved by sampling mini-batches from \mathcal{D} rather than processing the whole dataset on every iteration. In case of a single sample per minibatch, the iterations take the form

$$\mathbf{w}_{t+1} \leftarrow \mathbf{w}_t + \alpha_t \mathbf{d}_t \tag{3.7}$$

where $\alpha_t > 0$ is a learning rate and \mathbf{d}_t is a descent direction obtained from the gradient. In general, we have $\mathbf{d}_t = -\mathbf{C}_t \mathbf{g}_t$ where \mathbf{C}_t is a preconditioning matrix and $\mathbf{g} \triangleq \nabla_w \mathcal{L}$ is the gradient of the loss function. Note that we use the symbol \mathbf{C} instead of \mathbf{D} in order to highlight the fact that the matrix need not be diagonal and could actually be fully dense. Setting $\mathbf{C}_t = \mathbf{I}$ yields the basic Stochastic Gradient Descent (SGD) update [35]. In practice, the preferred training algorithm is often an accelerated version of SGD.

In this paper we investigate an alternative approach based on approximate second-order information: by defining the Hessian matrix of the loss function as $\mathbf{H} \triangleq \nabla_w^2 \mathcal{L}$ we set $\mathbf{C}_t \approx \mathbf{H}_t^{-1}$. This approach, if implemented naively, suffers from three drawbacks: (a) one needs to compute second-order derivatives with respect to \mathbf{w} ; (b) \mathbf{C}_t has to be positive-definite; and (c) a linear system $\mathbf{d} = -\mathbf{H}_t^{-1} \mathbf{g}$ must be solved, which scales cubically with the dimension of \mathbf{w} . These issues and the fact that \mathbf{w} is of rather large dimension have made the mentioned second-order method practically irrelevant in ML applications. Indeed, in many ML and RL applications, \mathbf{w} can be extremely high-dimensional, e.g., in case the function f_w is a large neural network, which explains why accelerated first-order methods are usually preferred.

While these observations seem to rule out second-order methods for ML applications, our main contribution is to show that one can develop algorithms which use approximate second-order information which have essentially the same per-iterate computational cost as SGD. To that end, we will derive the so-called Gauss-Newton Hessian approximation for incremental algorithms of the SGD family and prove that the update takes a very simple form.

3.3 Gauss-Newton Hessian Approximation

The special structure of the loss function (3.6) can be leveraged to derive an approximation of the exact Hessian which is restricted to least-squares problems (and generalizations thereof, as mentioned before and discussed in [36]) yielding fast convergence and not requiring the computation of second-order derivatives. To that end, we observe that the Hessian of Problem (3.1) reads

$$\mathbf{H} = \mathbf{J}^\top \mathbf{J} + \sum_{i=1}^N r_w^{(i)} \nabla_w^2 r_w^{(i)}, \tag{3.8}$$

where the Jacobian $\mathbf{J} \in \mathbb{R}^{N \times m}$ of the residual vector is $\mathbf{J} = \nabla_w \mathbf{r}_w^\top$. The idea behind the Gauss-Newton Hessian approximation is to neglect the second term in (3.8), to obtain

$$\mathbf{H}^{\text{GN}} = \mathbf{J}^\top \mathbf{J}. \tag{3.9}$$

From an intuitive point of view, one can see that this approximation is accurate as long as the residuals $\mathbf{r}_{\mathbf{w}}$ are small, since this makes the contribution of the second term in (3.8) small compared to the contribution of the first term. Note that this is the case when the fit is good, i.e., it is a situation that is expected to occur in learning problems. For more details we refer to [30] and references therein.

Since the gradient of the loss function reads $\mathbf{g}_t = \mathbf{J}_t^\top \mathbf{r}_{\mathbf{w}_t}$, by selecting $\mathbf{C}_t = (\mathbf{H}_t^{\text{GN}})^{-1} = (\mathbf{J}_t^\top \mathbf{J}_t)^{-1}$, we obtain the Gauss-Newton update

$$\mathbf{w}_{t+1} \leftarrow \mathbf{w}_t - \alpha_t \left(\mathbf{J}_t^\top \mathbf{J}_t \right)^{-1} \mathbf{J}_t^\top \mathbf{r}_{\mathbf{w}_t}. \quad (3.10)$$

Note that this is equivalent to $\mathbf{w}_{t+1} \leftarrow \mathbf{w}_t + \alpha_t \mathbf{d}_t^{\text{GN}}$, with

$$-\mathbf{d}_t^{\text{GN}} := \arg \min_{\Delta \mathbf{w}} \frac{1}{2} \left\| \mathbf{r}_{\mathbf{w}_t} + \nabla_{\mathbf{w}} \mathbf{r}_{\mathbf{w}_t}^\top \Delta \mathbf{w} \right\|_2^2. \quad (3.11)$$

The Gauss-Newton step (3.10) solves issues (a) and, partially, (b), since no second-order derivatives need to be computed and the Hessian approximation is positive semi-definite by construction. A positive-definite Hessian approximation can easily be obtained from \mathbf{H}^{GN} , e.g., by adding to it a small constant times the identity matrix. This approach is called Levenberg-Marquardt [30] and is often used in practice. As we will discuss later, our approach will not require this additional regularization, as the obtained step will implicitly guarantee that a positive definite Gauss-Newton approximation is used, which provides, in some sense, an optimal regularization.

The Gauss-Newton update, however, still potentially suffers from issue (c), i.e., the need to solve a linear system, which can be of cubic complexity. Before discussing our solution to (c), we would like to mention the method called Stochastic Gauss-Newton (SGN) proposed by [12], which consists in coupling the Gauss-Newton approximation with conjugate gradient iterations to approximately solve the linear system to a sufficient accuracy. Note that the complexity of CG is $\mathcal{O}(Cm^2)$ where C is the number of CG iterations and m the parameter dimension [30]. While this approach is very promising for batch algorithms, we will focus next on incremental algorithms of the form (3.7), for which we will obtain essentially the same complexity as SGD.

3.4 Incremental Gauss-Newton Derivation

In this subsection, we focus on the specific case of incremental algorithms, in which a single sample is processed at every iterate, i.e., $N = 1$, and at every time t a fitting problem is solved in which

$$\mathbf{r}_{\mathbf{w}}(\mathbf{y}, \mathbf{f}_{\mathbf{w}}(\mathbf{x})) = r_{\mathbf{w}}(y_t, f_{\mathbf{w}}(\mathbf{x}_t)) = r_{\mathbf{w}}^{(t)}. \quad (3.12)$$

Throughout this section, we will simplify the notation and drop the sample index since it coincides with the parameter index: $r_{\mathbf{w}_t} = r_{\mathbf{w}_t}^{(t)}$. The loss function then reads $\mathcal{L}(r_{\mathbf{w}}) = \frac{1}{2} r_{\mathbf{w}}^2$, and the Gauss-Newton direction is defined as

$$-\mathbf{d}_t^{\text{GN}} := \arg \min_{\Delta \mathbf{w}} \frac{1}{2} \left\| r_{\mathbf{w}_t} + \nabla_{\mathbf{w}} r_{\mathbf{w}_t}^\top \Delta \mathbf{w} \right\|_2^2. \quad (3.13)$$

Since the residual r is a scalar, its gradient is a vector, Problem (3.13) has infinitely many solutions, and the step cannot be computed as in (3.10) because

$$\mathbf{H}_t^{\text{GN}} = \mathbf{J}_t^\top \mathbf{J}_t = \nabla_{\mathbf{w}} r_{\mathbf{w}_t} \nabla_{\mathbf{w}} r_{\mathbf{w}_t}^\top$$

is rank 1 and, hence, not invertible. In order to tackle this issue, we compute the Gauss-Newton step by solving the following problem instead

$$-\mathbf{d}_t^{\text{GN}} = \arg \min_{\Delta \mathbf{w}} \frac{1}{2} \|r_{\mathbf{w}_t} + \nabla_{\mathbf{w}} r_{\mathbf{w}_t}^\top \Delta \mathbf{w}\|_2^2 + \frac{1}{2} \|\mathbf{Z}_t^\top \Delta \mathbf{w}\|_2^2, \quad (3.14)$$

with \mathbf{Z}_t the null-space of the residual function gradient, i.e., $\nabla_{\mathbf{w}} r_{\mathbf{w}_t}^\top \mathbf{Z}_t = 0$, $\mathbf{Z}_t^\top \mathbf{Z}_t = \mathbf{I}$.

We first recall the following useful result.

Lemma 3.1. *The solution of Problem (3.14) is also optimal for Problem (3.13).*

Proof. The optimality conditions of (3.14) read

$$\nabla_{\mathbf{w}} r_{\mathbf{w}_t} \left(r_{\mathbf{w}_t} + \nabla_{\mathbf{w}} r_{\mathbf{w}_t}^\top \Delta \mathbf{w} \right) + \mathbf{Z}_t \mathbf{Z}_t^\top \Delta \mathbf{w} = 0. \quad (3.15)$$

By decomposing the solution of (3.14) as

$$\Delta \mathbf{w} = -\mathbf{d}_t^{\text{GN}} = \mathbf{Y}_t \Delta \mathbf{w}^Y + \mathbf{Z}_t \Delta \mathbf{w}^Z,$$

with $\mathbf{Y}_t^\top \mathbf{Y}_t = \mathbf{I}$, $\mathbf{Z}_t^\top \mathbf{Y}_t = 0$, we have that the optimality conditions of (3.14) further become

$$\nabla_{\mathbf{w}} r_{\mathbf{w}_t} r_{\mathbf{w}_t} + \nabla_{\mathbf{w}} r_{\mathbf{w}_t} \nabla_{\mathbf{w}} r_{\mathbf{w}_t}^\top \mathbf{Y}_t \Delta \mathbf{w}^Y + \mathbf{Z}_t \Delta \mathbf{w}^Z = 0.$$

By premultiplying this equation with \mathbf{Z}_t^\top we obtain $\mathbf{Z}_t^\top \mathbf{Z}_t \Delta \mathbf{w}^Z = \Delta \mathbf{w}^Z = 0$, such that

$$\nabla_{\mathbf{w}} r_{\mathbf{w}_t} r_{\mathbf{w}_t} + \nabla_{\mathbf{w}} r_{\mathbf{w}_t} \nabla_{\mathbf{w}} r_{\mathbf{w}_t}^\top \mathbf{Y}_t \Delta \mathbf{w}^Y = 0,$$

and the optimal solution of (3.14) is $\Delta \mathbf{w} = \mathbf{Y}_t \Delta \mathbf{w}^Y$.

Since $\mathbf{Z}_t^\top \mathbf{Y}_t = 0$, using (3.15) we obtain

$$\nabla_{\mathbf{w}} r_{\mathbf{w}_t} \left(r_{\mathbf{w}_t} + \nabla_{\mathbf{w}} r_{\mathbf{w}_t}^\top \Delta \mathbf{w} \right) = 0,$$

which are the optimality conditions of (3.13), such that $\Delta \mathbf{w} = \mathbf{Y}_t \mathbf{w}_t^Y$ is also optimal for (3.11). \square

As it is formulated now, it is not clear that Problem (3.14) can be solved efficiently. Additionally, it seems necessary to compute the null space \mathbf{Z} , which is computationally demanding. However, as we prove in the next theorem, one does not need to compute the null space \mathbf{Z} and the solution to (3.14) can actually be obtained very cheaply.

Theorem 3.2. *The solution of Problem (3.14) is given by*

$$-\mathbf{d}_t^{\text{GN}} = \Delta \mathbf{w} = -\xi \nabla_{\mathbf{w}} r_{\mathbf{w}_t} r_{\mathbf{w}_t}, \quad (3.16)$$

with scalar ξ given by

$$\xi = \xi^{\text{GN}} = \frac{1}{\nabla_{\mathbf{w}} r_{\mathbf{w}_t}^\top \nabla_{\mathbf{w}} r_{\mathbf{w}_t}}.$$

Proof. By replacing (3.16) in (3.15) we obtain

$$\nabla_{\mathbf{w}} r_{\mathbf{w}_t} r_{\mathbf{w}_t} - \nabla_{\mathbf{w}} r_{\mathbf{w}_t} \frac{\nabla_{\mathbf{w}} r_{\mathbf{w}_t}^\top \nabla_{\mathbf{w}} r_{\mathbf{w}_t}}{\nabla_{\mathbf{w}} r_{\mathbf{w}_t}^\top \nabla_{\mathbf{w}} r_{\mathbf{w}_t}} r_{\mathbf{w}_t} - \mathbf{Z}_t \mathbf{Z}_t^\top \xi \nabla_{\mathbf{w}} r_{\mathbf{w}_t} r_{\mathbf{w}_t} = 0.$$

By the definition of null space we have $\mathbf{Z}^\top \nabla_{\mathbf{w}} r_{\mathbf{w}} = 0$, thus, the last term is zero. Moreover, the fraction in the second term evaluates to 1, such that we obtain

$$\nabla_{\mathbf{w}} r_{\mathbf{w}_t} r_{\mathbf{w}_t} - \nabla_{\mathbf{w}} r_{\mathbf{w}_t} r_{\mathbf{w}_t} = 0.$$

Therefore, Equation (3.16) does solve (3.14). \square

The obtained result is of extreme interest, as it proves that, with respect to computing the simplest SGD step, in order to obtain a Gauss-Newton step one only needs to evaluate scalar ξ , which only requires one vector-vector multiplication and one scalar division. Therefore, the additional computational burden with respect to SGD is essentially negligible. Moreover, this update benefits from being an approximation of the exact second-order step and makes the algorithm less sensitive to scaling, as we will discuss later. Additionally, this result provides an elegant way to address not only issue (c), but also issue (b) without requiring any additional regularization. Note that parameter regularization can be introduced in the problem, if that is desirable, but it needs not be introduced merely for computational reasons. This approach is akin to performing a QR decomposition of \mathbf{J}_t^\top that suggests interesting extensions to cover the mini-batch case, which is the subject of ongoing research.

One final remark about Problem (3.14) is in order. By introducing the second term in the cost we restrict our step to modify the parameter \mathbf{w} only in directions that do reduce the loss function, while the parameter is left unchanged along directions for which the loss function is locally flat. This fact can be seen by observing that $\nabla_{\mathbf{w}} \mathcal{L} = r_{\mathbf{w}} \nabla_{\mathbf{w}} r_{\mathbf{w}}$ and all directions along which the loss function is flat are encoded in the null space \mathbf{Z} , as $\nabla_{\mathbf{w}} r_{\mathbf{w}}^\top \mathbf{Z} = 0$. In other words, the idea behind the introduction of this extra term in the cost is that, since only a single data point is processed at each step, the available information is restricted to a specific direction in the parameter space (as $\nabla_{\mathbf{w}} r_{\mathbf{w}}$ has rank 1) and formulation (3.14) guarantees that the step does not move in directions for which no information is available.

Let us now comment on the computation of the solution to Problem (3.14) using the result of Theorem 3.2. Seeing that for least-squares losses $r_{\mathbf{w}_t} = y_t - f_{\mathbf{w}_t}(\mathbf{x}_t)$, by the chain rule we obtain

$$\frac{\partial r_{\mathbf{w}}(y_t, f_{\mathbf{w}}(\mathbf{x}_t))}{\partial \mathbf{w}} = \frac{\partial r_{\mathbf{w}}(y_t, f_{\mathbf{w}})}{\partial f_{\mathbf{w}}} \frac{\partial f_{\mathbf{w}}(\mathbf{x}_t)}{\partial \mathbf{w}} = - \frac{\partial f_{\mathbf{w}}(\mathbf{x}_t)}{\partial \mathbf{w}}.$$

We can evaluate ξ as $\xi = \frac{1}{\nabla_{\mathbf{w}} r_{\mathbf{w}_t}^\top \nabla_{\mathbf{w}} r_{\mathbf{w}_t}} = \frac{1}{\nabla_{\mathbf{w}} f_{\mathbf{w}_t}^\top \nabla_{\mathbf{w}} f_{\mathbf{w}_t}}$, so that the parameter update reads

$$\mathbf{w}_{t+1} \leftarrow \mathbf{w}_t + \alpha_t \xi_t \nabla_{\mathbf{w}} f_{\mathbf{w}_t}(\mathbf{x}_t) (y_t - f_{\mathbf{w}_t}(\mathbf{x}_t)). \quad (3.17)$$

The only case in which the step is not defined is when $\nabla_{\mathbf{w}} r_{\mathbf{w}_t} = 0$. However, that can only happen at the optimal solution, i.e., $\mathbf{w}_t = \mathbf{w}^*$ in which case it is clear that the step should be 0.

Note that the Levenberg-Marquardt regularization with parameter ϵ can be straightforwardly introduced in our approach by modifying ξ_t as

$$\xi_t = \frac{1}{\nabla_{\mathbf{w}} r_{\mathbf{w}_t}^\top \nabla_{\mathbf{w}} r_{\mathbf{w}_t} + \epsilon} = \frac{1}{\nabla_{\mathbf{w}} f_{\mathbf{w}_t}^\top \nabla_{\mathbf{w}} f_{\mathbf{w}_t} + \epsilon}. \quad (3.18)$$

Algorithm 1 Incremental Gauss-Newton Descent (IGND)

- 1: **Input:** dataset \mathcal{D} , learning rate α , initial weights \mathbf{w}_0 , LM regularizer ϵ .
 - 2: **repeat**
 - 3: Sample $\langle y_t, \mathbf{x}_t \rangle$ from the dataset \mathcal{D}
 - 4: Calculate prediction $f_{\mathbf{w}}(\mathbf{x}_t)$ and its sensitivity $\nabla_{\mathbf{w}} f_{\mathbf{w}_t}$
 - 5: Calculate $\xi_t = 1 / (\nabla_{\mathbf{w}} f_{\mathbf{w}_t}^\top \nabla_{\mathbf{w}} f_{\mathbf{w}_t} + \epsilon)$
 - 6: Update weights according to Equation (3.17)
 - 7: **until** convergence conditions hold
 - 8: **Return** weights \mathbf{w}
-

We draft the IGND procedure in Algorithm 1. The generic form is already applicable to supervised learning tasks. RL algorithms require some minor adjustments that we discuss in Section 4.

We discuss next how our approach compares to some variations of SGD proposed in the literature. The main difference with a standard stochastic gradient descent is that we introduce a scaling factor ξ which is not a matrix but a scalar, such that neither a matrix factorization nor matrix-vector multiplications are required. In fact, the only additional computations with respect to SGD are a vector-vector multiplication, an addition and a division.

We ought to emphasize the similarities and differences between IGND and some variations of clipped GD (CGD) [50] and normalized GD (NGD) [27, 28] that can be written in the form of (3.16), with

$$\xi^{\text{CGD}} = \min \left\{ \frac{1}{\eta}, \frac{1}{\|\nabla_{\mathbf{w}} \mathcal{L}\|} \right\}, \quad \xi^{\text{NGD}} = \frac{1}{\|\nabla_{\mathbf{w}} \mathcal{L}\| + \beta}.$$

While CGD and NGD use the norm of the gradient of the loss function, i.e., $\|\nabla_{\mathbf{w}} \mathcal{L}\|$, IGND is calculated based on the squared norm of the gradient of the function approximator, i.e., $\|\nabla_{\mathbf{w}} f\|^2$. The crucial difference is that, while $\nabla_{\mathbf{w}} \mathcal{L}$ tends to 0 at convergence, such that algorithms that do rescaling using its norm become ill-conditioned, this is not the case when using $\nabla_{\mathbf{w}} f$. Moreover, the norm has to be squared in order to obtain the correct approximation of the Hessian, which does not become 0 at convergence in practice.

3.5 Scale Invariance of IGND

In this subsection we briefly consider the tabular case, as it is useful to provide further intuition on how the Gauss-Newton algorithm works. The tabular case consists in having one weight per feature with a feature vector being a one-hot encoded (OHE) vector indicating the position in the look-up table, such that $\mathbf{x} \in \{0, 1\}^m$ and $\sum_{j=1}^m \mathbf{x}_j = 1$. In this case, we have $f_{\mathbf{w}}(\mathbf{x}) = \mathbf{w}^\top \mathbf{x} = \mathbf{w}^{(j)} \mathbf{x}^{(j)} = \mathbf{w}^{(j)}$ where j is the index of a non-zero feature. Since \mathbf{x} is a OHE vector, only one weight is being updated per iteration. Thus, the standard SGD update is given by

$$\mathbf{w}_{t+1}^{(j)} \leftarrow \mathbf{w}_t^{(j)} + \alpha_t r_{\mathbf{w}_t}, \quad (3.19)$$

which, due to one-hot encoding, corresponds to the change in the approximator function

$$f_{\mathbf{w}_{t+1}}(\mathbf{x}_t^{(j)}) - f_{\mathbf{w}_t}(\mathbf{x}_t^{(j)}) = \alpha_t r_{\mathbf{w}_t} \mathbf{x}_t^{(j)} = \alpha_t r_{\mathbf{w}_t}. \quad (3.20)$$

In order to discuss the benefit of the IGND approach, let us consider the impractical but insightful case in which we multiply each feature by some fixed scalar $\phi^{(j)}$, such that

$$f_{\mathbf{w}}(\mathbf{x}^{(j)}) = \phi^{(j)} \mathbf{w}^{(j)} \mathbf{x}^{(j)} = \phi^{(j)} \mathbf{w}^{(j)}. \quad (3.21)$$

In this case, the standard SGD update becomes

$$\mathbf{w}_{t+1}^{(j)} \leftarrow \mathbf{w}_t^{(j)} + \alpha_t r_{\mathbf{w}_t} \phi^{(j)}, \quad (3.22)$$

which corresponds to the function update

$$f_{\mathbf{w}_{t+1}}(\mathbf{x}_t^{(j)}) - f_{\mathbf{w}_t}(\mathbf{x}_t^{(j)}) = \alpha_t r_{\mathbf{w}_t} \phi^{(j)} \mathbf{x}_t^{(j)} \phi^{(j)} = \alpha_t r_{\mathbf{w}_t} (\phi^{(j)})^2,$$

i.e., the introduction of coefficients ϕ does change the step taken by the algorithm, as the function updates are scaled by ϕ^2 . When using a GN update, however, one obtains

$$\mathbf{w}_{t+1}^{(j)} \leftarrow \mathbf{w}_t^{(j)} + \alpha_t \xi_t r_{\mathbf{w}_t} \phi^{(j)}. \quad (3.23)$$

Since by construction $\xi_t = (\phi^{(j)})^{-2}$, we obtain

$$\mathbf{w}_{t+1}^{(j)} \leftarrow \mathbf{w}_t^{(j)} + \alpha_t r_{\mathbf{w}_t} (\phi^{(j)})^{-1}, \quad (3.24)$$

which corresponds to the function update

$$f_{\mathbf{w}_{t+1}}(\mathbf{x}_t^{(j)}) - f_{\mathbf{w}_t}(\mathbf{x}_t^{(j)}) = \alpha_t r_{\mathbf{w}_t} (\phi^{(j)})^{-1} \mathbf{x}_t^{(j)} \phi^{(j)} = \alpha_t r_{\mathbf{w}_t}. \quad (3.25)$$

Therefore, we recover exactly the same update as with standard SGD in the non-scaled tabular case. These derivations provide useful insight into the mechanism governing the IGND update, as they show that this makes the algorithm insensitive to scaling in the linear case. While this is not fully true for the nonlinear case, as we are neglecting some second-order terms, the beneficial effect of IGND still remains, as the neglected terms are small when the fit is good, and the scaling is close to being exact [30]. Then, one can understand the IGND update as providing approximate rescaling of the gradients, which adapts to how the gradient scaling evolves through the iterates. To illustrate the impact of feature scaling on a concrete example we refer to Section 5.2.

3.6 IGND Convergence

In order to state the convergence theory for IGND in a simple manner, let us introduce a notation that highlights the relevant dependencies while keeping the expressions relatively simple. Let us define the loss of the training set as

$$\bar{\mathcal{L}}(\mathbf{w}) := \mathbb{E}_{\zeta} \left[\frac{1}{2} (r_{\mathbf{w}}(y, \mathbf{f}_{\mathbf{w}}(\mathbf{x})))^2 \right], \quad (3.26)$$

where $\zeta = \langle y, \mathbf{x} \rangle$ is a tuple of random variables y (a scalar target) and \mathbf{x} (a vector of features). Note that, in case we have a dataset \mathcal{D} from which ζ is sampled with uniform probability, we obtain

$$\bar{\mathcal{L}}(\mathbf{w}) = \mathcal{L}(\mathbf{r}_{\mathbf{w}}(\mathbf{y}, \mathbf{f}_{\mathbf{w}}(\mathbf{x}))). \quad (3.27)$$

As we solve the problem by sampling, we will write the sample gradient

$$\mathbf{g}(\mathbf{w}, \zeta_i) := \nabla_{\mathbf{w}} \mathcal{L}(y_i, \mathbf{f}_{\mathbf{w}}(\mathbf{x}_i)), \quad (3.28)$$

which is an unbiased estimator of the true loss gradient, which satisfies $\nabla \bar{\mathcal{L}}(\mathbf{w}) = \mathbb{E}_{\zeta} [\mathbf{g}(\mathbf{w}, \zeta)]$. For the sake of clarity, we will make the dependence of ξ on \mathbf{w} and ζ explicit, i.e., we will write $\xi(\mathbf{w}, \zeta)$.

In the following, we will prove convergence of Algorithm 1 by adopting similar arguments as in standard SGD convergence proofs. In particular, we will adapt the arguments used in [2], which are based on proving that

$$\lim_{t \rightarrow \infty} \mathbb{E}_{\zeta} [\|\nabla \bar{\mathcal{L}}(\mathbf{w}_t)\|_2^2] = 0. \quad (3.29)$$

Note that we take the expected value with respect to ζ since \mathbf{w}_t does depend on the drawn samples of variable ζ , even though we do not make this dependence explicit for the sake of keeping notation simple.

In order to prove the desired result, we introduce next some assumptions and prove first some intermediate results.

Assumption 3.1. *The gradient norm of the function approximator $f_{\mathbf{w}}$ is bounded, i.e.,*

$$\|\nabla f_{\mathbf{w}}\|_2^2 \leq Q. \quad (3.30)$$

Assumption 3.1 entails that at each step $\xi(\mathbf{w}_t, \zeta_t)$ is a bounded positive scalar, i.e., $\xi(\mathbf{w}_t, \zeta_t) \in \left(\frac{1}{Q+\epsilon}, \frac{1}{\epsilon}\right)$. Note that this mild assumption is sometimes not made explicit, though it is always necessary in order to guarantee that any gradient-based method delivers a well-defined step.

Assumption 3.2. *The loss function $\bar{\mathcal{L}}(\mathbf{w}) : \mathbb{R}^m \rightarrow \mathbb{R}$ is continuously differentiable and the gradient function $\nabla \bar{\mathcal{L}} : \mathbb{R}^m \rightarrow \mathbb{R}^m$, is Lipschitz continuous with Lipschitz constant L , i.e., for all $\{\mathbf{w}, \bar{\mathbf{w}}\} \subset \mathbb{R}^m$*

$$\|\nabla \bar{\mathcal{L}}(\mathbf{w}) - \nabla \bar{\mathcal{L}}(\bar{\mathbf{w}})\|_2 \leq L \|\mathbf{w} - \bar{\mathbf{w}}\|_2. \quad (3.31)$$

An immediate consequence of Assumption 3.2 is that, for all $\{\mathbf{w}, \bar{\mathbf{w}}\} \subset \mathbb{R}^m$ we have

$$\bar{\mathcal{L}}(\mathbf{w}) \leq \bar{\mathcal{L}}(\bar{\mathbf{w}}) + \nabla \bar{\mathcal{L}}(\bar{\mathbf{w}})^{\top} (\mathbf{w} - \bar{\mathbf{w}}) + \frac{1}{2} L \|\mathbf{w} - \bar{\mathbf{w}}\|_2^2. \quad (3.32)$$

Lemma 3.3. *Under Assumption 3.2, the iterates of Algorithm 1 satisfy the following inequality for all $t \in \mathbb{N}$:*

$$\mathbb{E}_{\zeta_t} [\bar{\mathcal{L}}(\mathbf{w}_{t+1})] - \bar{\mathcal{L}}(\mathbf{w}_t) \leq -\alpha_t \nabla \bar{\mathcal{L}}(\mathbf{w}_t)^{\top} \mathbb{E}_{\zeta_t} [\xi(\mathbf{w}_t, \zeta_t) \mathbf{g}(\mathbf{w}_t, \zeta_t)] + \frac{1}{2} \alpha_t^2 L \mathbb{E}_{\zeta_t} \|\xi(\mathbf{w}_t, \zeta_t) \mathbf{g}(\mathbf{w}_t, \zeta_t)\|_2^2. \quad (3.33)$$

Proof. We first recall that the IGND iterate is

$$\mathbf{w}_{t+1} \leftarrow \mathbf{w}_t - \alpha_t \xi(\mathbf{w}_t, \zeta_t) \mathbf{g}(\mathbf{w}_t, \zeta_t). \quad (3.34)$$

Expanding Equation (3.32) yields

$$\begin{aligned} \bar{\mathcal{L}}(\mathbf{w}_{t+1}) - \bar{\mathcal{L}}(\mathbf{w}_t) &\leq \nabla \bar{\mathcal{L}}(\mathbf{w}_t)^{\top} (\mathbf{w}_{t+1} - \mathbf{w}_t) + \frac{1}{2} L \|\mathbf{w}_{t+1} - \mathbf{w}_t\|_2^2 \\ &\leq -\alpha_t \nabla \bar{\mathcal{L}}(\mathbf{w}_t)^{\top} (\xi(\mathbf{w}_t, \zeta_t) \mathbf{g}(\mathbf{w}_t, \zeta_t)) + \frac{1}{2} \alpha_t^2 L \|\xi(\mathbf{w}_t, \zeta_t) \mathbf{g}(\mathbf{w}_t, \zeta_t)\|_2^2. \end{aligned} \quad (3.35)$$

The result is then obtained by taking expectations with respect to ζ_t and remembering that \mathbf{w}_{t+1} does depend on ζ_t , while \mathbf{w}_t and α_t do not. \square

This lemma proves that the expected decrease in the loss function yielded by the step t is bounded above by a quantity involving two terms: (i) the inner product between the expected directional derivative of \mathcal{L} at \mathbf{w}_t and the expectation of $-\xi(\mathbf{w}_t, \zeta_t)\mathbf{g}(\mathbf{x}_t, \zeta_t)$; and (ii) the second moment of $\xi(\mathbf{w}_t, \zeta_t)\mathbf{g}(\mathbf{x}_t, \zeta_t)$. Our next assumption (similarly to the SGD convergence proof) concerns both terms, the second of which involves the variance of $\xi(\mathbf{w}_t, \zeta_t)\mathbf{g}(\mathbf{w}_t, \zeta_t)$, i.e.:

$$\mathbb{V}_{\zeta_t}[\xi(\mathbf{w}_t, \zeta_t)\mathbf{g}(\mathbf{w}_t, \zeta_t)] := \mathbb{E}_{\zeta_t}[\|\xi(\mathbf{w}_t, \zeta_t)\mathbf{g}(\mathbf{w}_t, \zeta_t)\|_2^2] - \|\mathbb{E}_{\zeta_t}[\xi(\mathbf{w}_t, \zeta_t)\mathbf{g}(\mathbf{w}_t, \zeta_t)]\|_2^2. \quad (3.36)$$

Before introducing the next assumption, we observe that it slightly differs from the one used in [2]. In case ξ were estimated by drawing an independent sample of ζ , then the assumptions of [2] could be directly used and the proof would only require minor adaptations. We leave the investigation of that algorithm for future research, as the associated computational burden is significantly higher compared to IGND.

Assumption 3.3. *The following hold:*

- (a) *The sequence of iterates $\{\mathbf{w}_t\}$ is contained in an open set over which $\bar{\mathcal{L}}$ is bounded below by a scalar $\bar{\mathcal{L}}_{\text{inf}}$, i.e., for all t*

$$\bar{\mathcal{L}}(\mathbf{w}_t) \geq \bar{\mathcal{L}}_{\text{inf}}. \quad (3.37)$$

- (b) *There exist scalars $\mu_G \geq \mu > 0$ such that, for all $t \in \mathbb{N}$,*

$$\nabla \bar{\mathcal{L}}(\mathbf{w}_t)^\top \mathbb{E}_{\zeta_t}[\xi(\mathbf{w}_t, \zeta_t)\mathbf{g}(\mathbf{w}_t, \zeta_t)] \geq \mu \|\nabla \bar{\mathcal{L}}(\mathbf{w}_t)\|_2^2, \quad (3.38)$$

$$\|\mathbb{E}_{\zeta_t}[\xi(\mathbf{w}_t, \zeta_t)\mathbf{g}(\mathbf{w}_t, \zeta_t)]\|_2 \leq \mu_G \|\nabla \bar{\mathcal{L}}(\mathbf{w}_t)\|_2. \quad (3.39)$$

- (c) *There exist scalars $M \geq 0$ and $M_V \geq 0$ such that, for all $t \in \mathbb{N}$,*

$$\mathbb{V}_{\zeta_t}[\xi(\mathbf{w}_t, \zeta_t)\mathbf{g}(\mathbf{w}_t, \zeta_t)] \leq M + M_V \|\nabla \bar{\mathcal{L}}(\mathbf{w}_t)\|_2^2. \quad (3.40)$$

In combination Equation (3.36) and Assumption 3.3 entail that the variance of $\xi(\mathbf{w}_t, \zeta_t)\mathbf{g}(\mathbf{w}_t, \zeta_t)$ satisfies

$$\mathbb{E}_{\zeta_t}[\|\xi(\mathbf{w}_t, \zeta_t)\mathbf{g}(\mathbf{w}_t, \zeta_t)\|_2^2] \leq M + M_G \|\nabla \bar{\mathcal{L}}(\mathbf{w}_t)\|_2^2 \quad (3.41)$$

with $M_G := M_V + \mu_G^2 \geq \mu^2 > 0$.

By applying Equation (3.41) together with Lemma 3.3, we derive Lemma 3.4.

Lemma 3.4. *Under Assumptions 3.2 and 3.3, the iterates of Algorithm 1 satisfy the following inequalities for all $t \in \mathbb{N}$:*

$$\mathbb{E}_{\zeta_t}[\bar{\mathcal{L}}(\mathbf{w}_{t+1})] - \bar{\mathcal{L}}(\mathbf{w}_t) \leq -\left(\mu - \frac{1}{2}\alpha_t LM_G\right)\alpha_t \|\nabla \bar{\mathcal{L}}(\mathbf{w}_t)\|_2^2 + \frac{1}{2}\alpha_t^2 LM. \quad (3.42)$$

Proof. The result is obtained by relying on Lemma 3.3 and bounding the terms using Assumption 3.3 as follows

$$\begin{aligned} \mathbb{E}_{\zeta_t}[\bar{\mathcal{L}}(\mathbf{w}_{t+1})] - \bar{\mathcal{L}}(\mathbf{w}_t) &\stackrel{(3.33)}{\leq} -\alpha_t \nabla \bar{\mathcal{L}}(\mathbf{w}_t)^\top \mathbb{E}_{\zeta_t}[\xi(\mathbf{w}_t, \zeta_t)\mathbf{g}(\mathbf{w}_t, \zeta_t)] + \frac{1}{2}\alpha_t^2 L \mathbb{E}_{\zeta_t}[\|\xi(\mathbf{w}_t, \zeta_t)\mathbf{g}(\mathbf{w}_t, \zeta_t)\|_2^2] \\ &\stackrel{(3.38), (3.41)}{\leq} -\mu\alpha_t \|\nabla \bar{\mathcal{L}}(\mathbf{w}_t)\|_2^2 + \frac{1}{2}\alpha_t^2 L (M + M_G \|\nabla \bar{\mathcal{L}}(\mathbf{w}_t)\|_2^2) \\ &\leq -\left(\mu - \frac{1}{2}\alpha_t LM_G\right)\alpha_t \|\nabla \bar{\mathcal{L}}(\mathbf{w}_t)\|_2^2 + \frac{1}{2}\alpha_t^2 LM. \end{aligned}$$

□

Finally, in order to complete the proof one last assumption is needed on the stepsize.

Assumption 3.4. *The learning rate sequence $\{\alpha_t\}$ follows the Robbins-Monro conditions [3, 35]:*

$$\sum_{t=1}^{\infty} \alpha_t = \infty, \quad \sum_{t=1}^{\infty} \alpha_t^2 < \infty. \quad (3.43)$$

We are now ready to state the convergence theorem whose proof is the one given in [2]. The main difference with [2] is in how we obtained the bounds above.

Theorem 3.5 (From [2]). *Under Assumptions 3.1, 3.2, 3.3 and 3.4, it holds that*

$$\lim_{T \rightarrow \infty} \mathbb{E}_{\zeta_0 \rightarrow \infty} \left[\sum_{t=1}^T \alpha_t \|\nabla \bar{\mathcal{L}}(\mathbf{w}_t)\|_2^2 \right] < \infty, \quad (3.44)$$

and, therefore,

$$\lim_{T \rightarrow \infty} \mathbb{E}_{\zeta_0 \rightarrow \infty} \left[\frac{1}{A_T} \sum_{t=1}^T \alpha_t \|\nabla \bar{\mathcal{L}}(\mathbf{w}_t)\|_2^2 \right] = 0. \quad (3.45)$$

where $A_T := \sum_{t=1}^T \alpha_t$.

Proof. The second condition in Assumption 3.4 ensures that $\lim_{t \rightarrow \infty} \alpha_t \rightarrow 0$, which entails that, without loss of generality, we can assume $\alpha_t LM_G \leq \mu$ for all $t \in \mathbb{N}$.

Using (3.37) we have

$$\begin{aligned} & \bar{\mathcal{L}}_{\inf} - \mathbb{E}_{\zeta_0 \rightarrow \infty} [\bar{\mathcal{L}}(\mathbf{w}_1)] \\ & \leq \mathbb{E}_{\zeta_0 \rightarrow \infty} [\bar{\mathcal{L}}(\mathbf{w}_{T+1})] - \mathbb{E}_{\zeta_0 \rightarrow \infty} [\bar{\mathcal{L}}(\mathbf{w}_1)] \\ & \leq -\frac{1}{2}\mu \sum_{t=1}^T \alpha_t \mathbb{E}_{\zeta_0 \rightarrow \infty} [\|\nabla \bar{\mathcal{L}}(\mathbf{w}_t)\|_2^2] + \frac{1}{2}LM \sum_{t=1}^T \alpha_t^2, \end{aligned} \quad (3.46)$$

where we used the result of Lemma 3.4 recursively to obtain the second inequality. Dividing by $\mu/2$ and rearranging the terms, we obtain

$$\sum_{t=1}^T \alpha_t \mathbb{E}_{\zeta_0 \rightarrow \infty} [\|\nabla \bar{\mathcal{L}}(\mathbf{w}_t)\|_2^2] \leq \frac{2(\mathbb{E}_{\zeta_0 \rightarrow \infty} [\bar{\mathcal{L}}(\mathbf{w}_1)] - \bar{\mathcal{L}}_{\inf})}{\mu} + \frac{LM}{\mu} \sum_{t=1}^T \alpha_t^2. \quad (3.47)$$

By Assumption 3.4 the right-hand side of this inequality must converge to a finite limit as $T \rightarrow \infty$, which proves (3.44). Equation (3.45) immediately follows, since the first condition in Assumption 3.4 ensures that $A_T \rightarrow \infty$ as $T \rightarrow \infty$. □

Corollary 3.6 (From [2]). *Under the conditions of Theorem 3.5, if we further assume that the objective function $\bar{\mathcal{L}}$ is twice differentiable, and that the mapping $\mathbf{w} \mapsto \|\nabla \bar{\mathcal{L}}(\mathbf{w})\|_2^2$ has Lipschitz-continuous derivatives, then*

$$\lim_{t \rightarrow \infty} \mathbb{E} [\|\nabla \bar{\mathcal{L}}(\mathbf{w}_t)\|_2^2] = 0. \quad (3.48)$$

Proof. We define $G(\mathbf{w}) := \|\nabla\bar{\mathcal{L}}(\mathbf{w})\|_2^2$ and let L_G be the Lipschitz constant of $\nabla G(\mathbf{w}) = 2\nabla^2\bar{\mathcal{L}}(\mathbf{w})\nabla\bar{\mathcal{L}}(\mathbf{w})$. Then, by using Equation (3.32) adapted to G and replacing the weight difference with the IGND iteration (3.34) that generates it we have

$$\begin{aligned} & G(\mathbf{w}_{t+1}) - G(\mathbf{w}_t) \\ & \leq \nabla G(\mathbf{w}_t)^\top (\mathbf{w}_{t+1} - \mathbf{w}_t) + \frac{1}{2}L_G\|\mathbf{w}_{t+1} - \mathbf{w}_t\|_2^2 \end{aligned} \quad (3.49)$$

$$\leq -\alpha_t\nabla G(\mathbf{w}_t)^\top (\xi(\mathbf{w}_t, \zeta_t)\mathbf{g}(\mathbf{w}_t, \zeta_t)) + \frac{1}{2}\alpha_t^2L_G\|\xi(\mathbf{w}_t, \zeta_t)\mathbf{g}(\mathbf{w}_t, \zeta_t)\|_2^2. \quad (3.50)$$

Taking the expectation with respect to the distribution of ζ_t and recalling the definition of $\nabla G(\mathbf{w})$, we have

$$\begin{aligned} & \mathbb{E}_{\zeta_t}[G(\mathbf{w}_{t+1})] - G(\mathbf{w}_t) \\ & \leq -2\alpha_t\nabla\bar{\mathcal{L}}(\mathbf{w}_t)^\top\nabla^2\bar{\mathcal{L}}(\mathbf{w}_t)^\top\mathbb{E}_{\zeta_t}[\xi(\mathbf{w}_t, \zeta_t)\mathbf{g}(\mathbf{w}_t, \zeta_t)] + \frac{1}{2}\alpha_t^2L_G\mathbb{E}_{\zeta_t}[\|\xi(\mathbf{w}_t, \zeta_t)\mathbf{g}(\mathbf{w}_t, \zeta_t)\|_2^2]. \end{aligned} \quad (3.51)$$

Applying the Cauchy-Schwarz inequality yields

$$-2\alpha_t\nabla\bar{\mathcal{L}}(\mathbf{w}_t)^\top\nabla^2\bar{\mathcal{L}}(\mathbf{w}_t)^\top\mathbb{E}_{\zeta_t}[\xi(\mathbf{w}_t, \zeta_t)\mathbf{g}(\mathbf{w}_t, \zeta_t)] \leq 2\alpha_t\|\nabla\bar{\mathcal{L}}(\mathbf{w}_t)\|_2\|\nabla^2\bar{\mathcal{L}}(\mathbf{w}_t)\|_2\|\mathbb{E}_{\zeta_t}[\xi(\mathbf{w}_t, \zeta_t)\mathbf{g}(\mathbf{w}_t, \zeta_t)]\|_2.$$

As we showed earlier, it holds that

$$\begin{aligned} \|\mathbb{E}_{\zeta_t}[\xi(\mathbf{w}_t, \zeta_t)\mathbf{g}(\mathbf{w}_t, \zeta_t)]\|_2 & \leq \mu_G\|\nabla\bar{\mathcal{L}}(\mathbf{w}_t)\|_2, \\ \nabla^2\bar{\mathcal{L}}(\mathbf{w}_t) & \leq L. \end{aligned}$$

Using these results in combination with (3.51) we further obtain

$$\begin{aligned} & \mathbb{E}_{\zeta_t}[G(\mathbf{w}_{t+1})] - G(\mathbf{w}_t) \\ & \leq 2\alpha_tL\mu_G\|\nabla\bar{\mathcal{L}}(\mathbf{w}_t)\|_2^2 + \frac{1}{2}\alpha_t^2L_G\mathbb{E}_{\zeta_t}[\|\xi(\mathbf{w}_t, \zeta_t)\mathbf{g}(\mathbf{w}_t, \zeta_t)\|_2^2]. \end{aligned}$$

Limiting the second moment using Inequality (3.41) yields

$$\begin{aligned} & \mathbb{E}_{\zeta_t}[G(\mathbf{w}_{t+1})] - G(\mathbf{w}_t) \\ & \leq 2\alpha_tL\mu_G\|\nabla\bar{\mathcal{L}}(\mathbf{w}_t)\|_2^2 + \frac{1}{2}\alpha_t^2L_G(M + M_G\|\nabla\bar{\mathcal{L}}(\mathbf{w}_t)\|_2^2). \end{aligned} \quad (3.52)$$

By applying the expectation over all parameter updates, we finally obtain

$$\begin{aligned} & \mathbb{E}_{\zeta_{0 \rightarrow \infty}}[G(\mathbf{w}_{t+1})] - \mathbb{E}_{\zeta_{0 \rightarrow \infty}}[G(\mathbf{w}_t)] \\ & \leq 2\alpha_tL\mu_G\mathbb{E}_{\zeta_{0 \rightarrow \infty}}[\|\nabla\bar{\mathcal{L}}(\mathbf{w}_t)\|_2^2] + \frac{1}{2}\alpha_t^2L_G(M + M_G\mathbb{E}_{\zeta_{0 \rightarrow \infty}}[\|\nabla\bar{\mathcal{L}}(\mathbf{w}_t)\|_2^2]). \end{aligned} \quad (3.53)$$

By Theorem 3.5 the first component of this bound is the term of a convergent sum. Moreover, the second component of this bound is also the term of a convergent sum since $\sum_{k=1}^{\infty}\alpha_t^2$ converges and $\alpha_t^2 \leq \alpha_t$ for sufficiently large $t \in \mathbb{N}$, such that the result of Theorem 3.5 can be applied also to this

second term. Therefore, the right-hand side of (3.53) is the term of a convergent sum. Let us now define

$$S_T^+ = \sum_{t=1}^T \max(0, \mathbb{E}_{\zeta_0 \rightarrow \infty} [G(\mathbf{w}_{t+1})] - \mathbb{E}_{\zeta_0 \rightarrow \infty} [G(\mathbf{w}_t)]), \quad (3.54)$$

$$S_T^- = \sum_{t=1}^T \max(0, \mathbb{E}_{\zeta_0 \rightarrow \infty} [G(\mathbf{w}_t)] - \mathbb{E}_{\zeta_0 \rightarrow \infty} [G(\mathbf{w}_{t+1})]). \quad (3.55)$$

Since the right hand side in (3.53) is positive and forms a convergent sum, the non-decreasing sequence S_T^+ is upper bounded and therefore converges. Since, for any $T \in \mathbb{N}$, one has

$$\mathbb{E}_{\zeta_0 \rightarrow \infty} [G(\mathbf{w}_T)] = G(\mathbf{w}_0) + S_T^+ - S_T^- \geq 0,$$

the non-decreasing sequence S_T^- must also be upper bounded and therefore also converges. Therefore, $\mathbb{E}_{\zeta_0 \rightarrow \infty} [G(\mathbf{w}_T)]$ converges and its limit must be zero, which entails $\lim_{t \rightarrow \infty} \mathbb{E}[\|\nabla \bar{\mathcal{L}}(\mathbf{w}_t)\|_2^2] = 0$. \square

4 IGND for Machine Learning Applications

The IGND algorithm presented above has a generic form and can be adapted to various machine learning problems.

4.1 Supervised Learning

While there do exist many possible formulations of supervised learning problems, in this paper we restrict our attention to least-squares regression for the sake of simplicity. In this case, the formulas provided above already deliver all the necessary ingredients to run IGND.

4.2 Value-Based Reinforcement Learning

We provide next a quick overview of how IGND can be adapted to value-based RL formulations. The intent is not to cover all possible formulations, but rather to provide the information necessary to understand how the algorithm can be integrated with value-based RL methods.

We consider environments structured as a Markov Decision Process (MDP) $\mathcal{M} = \langle \mathcal{S}, \mathcal{A}, T, r, \gamma \rangle$ with the state space \mathcal{S} ; the action space \mathcal{A} ; the stochastic transition function $T(s'|s, a) = \mathbb{P}[S_{t+1} = s' | S_t = s, A_t = a]$, which defines the probability of transitioning from state s to state s' while taking action a ; the reward function $r(s, a)$ and the discount factor $\gamma \in [0, 1]$.

The action-value function $q^\pi(s, a) : \mathcal{S} \times \mathcal{A} \rightarrow \mathbb{R}$ under policy π is defined as the sum of discounted future rewards

$$q^\pi(s, a) = \mathbb{E}_\pi \left[\sum_{t=0}^{\infty} \gamma^t r(S_t, A_t) \mid S_0 = s, A_0 = a \right], \quad (4.1)$$

where the expectation is taken over the trajectories generated under policy π . Value-based methods in reinforcement learning aim at finding the optimal Q-function $q^*(s, a)$ by solving $q^*(s, a) = \max_\pi q^\pi(s, a)$. Since this problem is infinite-dimensional, the problem is made tractable by replacing the actual action-value function by a parametric approximation $q_{\mathbf{w}}(s, a)$ with finite-dimensional parameter vector \mathbf{w} , e.g., a neural network. Then the problem becomes $\max_{\mathbf{w}} q_{\mathbf{w}}(s, a)$.

In order to evaluate \mathbf{w} for a given policy π we minimize the squared loss of the true Q-function $q^*(s, a)$ and the approximate Q-function $q_{\mathbf{w}}(s, a)$

$$\mathcal{L}(\mathbf{r}_{\mathbf{w}}) = \frac{1}{2} \mathbb{E}_{\mu} \left[(q^*(s, a) - q_{\mathbf{w}}(s, a))^2 \right], \quad (4.2)$$

where the expectation is taken over the distribution μ of states and actions corresponding to a given policy, e.g., the ϵ -greedy policy related to $q_{\mathbf{w}_t}(\cdot, a)$ [39]. In practice, this problem is solved by taking the empirical expectation over trajectories sampled using a given policy which ensures sufficient exploration.

Since the true value of $q^*(s, a)$ is unknown, a common approach is to approximate it with off-policy one-step temporal difference return (also known as a TD target) thus obtaining the incremental update as

$$\arg \min_{\mathbf{w}} \frac{1}{2} [y_t - q_{\mathbf{w}}(S_t, A_t)]^2, \quad (4.3)$$

where

$$y_t = R_{t+1} + \gamma \max_{a'} q_{\mathbf{w}_t}(S_{t+1}, a'), \quad (4.4)$$

$$f_{\mathbf{w}}(\mathbf{x}_t) = q_{\mathbf{w}}(S_t, A_t), \quad \mathbf{x}_t = [s_t^\top \ a_t^\top]^\top. \quad (4.5)$$

Note that, as opposed to $f_{\mathbf{w}}(\mathbf{x}_t)$, the TD target y_t is not a function of the optimization variable \mathbf{w} , though it does depend on the current parameter value \mathbf{w}_t . The minimization of (4.3) is referred to as stochastic semi-gradient method [39]. The gradient of $\mathcal{L}(\mathbf{r}(\mathbf{w}))$ with respect to \mathbf{w} reads

$$\nabla_{\mathbf{w}} \mathcal{L} = -(y_t - q_{\mathbf{w}}(S_t, A_t)) \nabla q_{\mathbf{w}}(S_t, A_t). \quad (4.6)$$

By observing that $y_t - q_{\mathbf{w}}(S_t, A_t)$ is the TD error δ_t we obtain the well-known Q-learning update

$$\mathbf{w}_{t+1} \leftarrow \mathbf{w}_t + \alpha_t \delta_t \nabla q_{\mathbf{w}}. \quad (4.7)$$

A SARSA update is obtained if in (4.4) $\max_{a'}$ is replaced by sampling the next action a' from the current policy. Other popular variants of these algorithms are not detailed here, but a complete overview can be found in [11, 39] and references therein.

The Gauss-Newton approach we proposed in Section 3 can be deployed in reinforcement learning by noting that Equations (4.4)-(4.5) relate the action-value function approximation $q_{\mathbf{w}}(s, a)$ to function $f_{\mathbf{w}}(\mathbf{x}_t)$ and the TD-target to the target y_t . We can then define what we call the Gauss-Newton Q-learning (IGNDQ) update as

$$\mathbf{w}_{t+1} \leftarrow \mathbf{w}_t + \alpha_t \xi_t \delta_t \nabla q_{\mathbf{w}} \quad (4.8)$$

with the full procedure is sketched in Algorithm 2.

4.3 Gauss-Newton Policy Iteration for LQR

While the methods presented above could also be used for LQR, we present an additional one in order to show that our algorithm applies to many different settings. LQR considers a discrete time-invariant linear system with continuous states $\mathcal{S} \in \mathbb{R}^{n_s}$ and actions $\mathcal{A} \in \mathbb{R}^{n_a}$. For stochastic systems, the transition function is defined as

$$T(s, a) = \mathbf{A}s + \mathbf{B}a + e, \quad (4.9)$$

Algorithm 2 Gauss-Newton Q-learning (IGNDQ)

- 1: **Input:** learning rate α , discount factor γ , target update frequency p , policy π , LM regularizer ϵ .
 - 2: Initialize Q-network $q_{\mathbf{w}}$ with random weights
 - 3: Copy weights into the target network $\bar{\mathbf{w}} \leftarrow \mathbf{w}$
 - 4: **for** episode = 1 to M **do**
 - 5: Initialize S_0
 - 6: **for** $t = 0$ to T **do**
 - 7: Choose action $A_t \sim \pi(S_t)$
 - 8: Execute action A_t and observe R_t, S_{t+1}
 - 9: Calculate TD target using the target network $y_t = R_t + \gamma \max_{a'} q_{\bar{\mathbf{w}}}(S_{t+1}, a')$
 - 10: Calculate Q-value $q_{\mathbf{w}}(S_t, A_t)$ and its sensitivity $\nabla_{\mathbf{w}} q_{\mathbf{w}}(S_t, A_t)$
 - 11: Calculate TD error $\delta_t = y_t - q_{\mathbf{w}}(S_t, A_t)$
 - 12: Calculate $\xi_t = 1 / (\nabla_{\mathbf{w}} q_{\mathbf{w}_t}^\top \nabla_{\mathbf{w}} q_{\mathbf{w}_t} + \epsilon)$
 - 13: Update weights according to equation (4.8)
 - 14: Every p steps copy weights into target network $\bar{\mathbf{w}} \leftarrow \mathbf{w}$
 - 15: **end for**
 - 16: **end for**
 - 17: **Return** weights \mathbf{w}
-

with system matrices $\mathbf{A} \in \mathbb{R}^{n_s \times n_s}$, $\mathbf{B} \in \mathbb{R}^{n_a \times n_s}$ and Gaussian noise $e \sim \mathcal{N}(0, \Sigma)$. The reward function is

$$r(s, a) = s^\top \mathbf{Q} s + a^\top \mathbf{R} a, \quad (4.10)$$

where $\mathbf{Q} \in \mathbb{R}^{n_s \times n_s}$ is negative semi-definite and $\mathbf{R} \in \mathbb{R}^{n_a \times n_a}$ is negative definite. The optimal value function and policy are:

$$v^*(s) = s^\top \mathbf{P} s + V_0, \quad \pi^*(s) = \mathbf{K} s, \quad (4.11)$$

where $\mathbf{P} \in \mathbb{R}^{n_s \times n_s}$ is a negative semi-definite matrix that defines the value function, $\mathbf{K} \in \mathbb{R}^{n_a \times n_s}$ is a state feedback matrix and $V_0 = \gamma(1 - \gamma)^{-1} \text{Tr}(\mathbf{P}\Sigma)$. In case the matrices \mathbf{A} , \mathbf{B} , \mathbf{Q} and \mathbf{R} are known the optimal solution can be found by solving discrete-time algebraic Riccati equations. For data-driven systems the standard Q-learning update (4.7) as well as the IGND update (4.8) can be incorporated into the policy iteration procedure of [4]. The algorithm relies on the fact that the Q-function for LQ problems is quadratic

$$q_{\pi}^*(s, a) = \begin{bmatrix} s \\ a \end{bmatrix}^\top \underbrace{\begin{bmatrix} \mathbf{M}_{ss} & \mathbf{M}_{sa} \\ \mathbf{M}_{as} & \mathbf{M}_{aa} \end{bmatrix}}_{\mathbf{M}} \begin{bmatrix} s \\ a \end{bmatrix} + c, \quad (4.12)$$

with the matrix \mathbf{M} and a constant c updated through the policy evaluation stage. During the policy improvement step the policy is updated as $\mathbf{K} = -\mathbf{M}_{aa}^{-1} \mathbf{M}_{as}$ (Algorithm 3).

5 Experiments

5.1 Supervised Learning

In this section we conduct several numerical simulations to assess the performance of IGND.

Algorithm 3 Generalized Policy Iteration for LQR

- 1: **Input:** initial stabilizing policy \mathbf{K}_0 , initial weights \mathbf{w}_0 , learning rate α , discount factor γ , tolerance $\eta = 10^{-8}$, LM regularizer ϵ .
 - 2: Set policy iteration counter $p = 1$
 - 3: **repeat**
 - 4: Given \mathbf{K}_{p-1} estimate the corresponding weights \mathbf{w} through a policy evaluation algorithm, eg. Algorithm 4
 - 5: Convert weights \mathbf{w} to a matrix \mathbf{M}
 - 6: **if** \mathbf{M}_{aa} is not positive-definite **then**
 - 7: **Return** Error
 - 8: **end if**
 - 9: Improve policy $\mathbf{K}_p = -\mathbf{M}_{aa}^{-1}\mathbf{M}_{as}$
 - 10: Set $p = p + 1$
 - 11: **until** $\|\mathbf{K}_p - \mathbf{K}_{p-1}\| < \eta$
 - 12: **Return** \mathbf{K}_p
-

California Housing consists of 20640 samples with 8 numerical features \mathbf{x} encoding relevant information, e.g., location, median income, etc.; and a real-valued target \mathbf{y} representing the median house value in California as recorded by the 1990 U.S. Census [31]. The full description of the features could be found at <https://developers.google.com/machine-learning/crash-course/california-housing-data-description>.

Diamonds is a dataset containing 53940 instances of 9 physical attributes (both numerical and categorical features \mathbf{x}) and prices (target \mathbf{y}) of diamonds [43]. The full description of the dataset could be found at <https://www.tensorflow.org/datasets/catalog/diamonds>.

For both problems we use as function approximator $f_{\mathbf{w}}$ a Feedforward Neural Network (FFNN) with 3 hidden layers of 32, 64 and 32 units followed by ReLU activation functions. The loss function is a least-squares function defined as (3.6). Both datasets are split into train and test sets in the proportion of 80/20 percent. Numerical features are scaled and categorical features are one-hot encoded.

We compare IGND and SGD, as well as Adam and IGND with Adam, where the gradients are scaled by ξ before being passed to the Adam algorithm. The learning rates are selected as the best performing α after the grid search in the logspace $\alpha \in [10^{-9}, 1]$. We evaluate the algorithms on the test set based on the Mean Absolute Percentage Error defined as ($\epsilon = 10^{-15}$)

$$E_{\text{MAPE}}(\mathbf{y}, \mathbf{f}_{\mathbf{w}}(\mathbf{x})) = \frac{1}{N} \sum_{i=1}^N \frac{|y_i - f_{\mathbf{w}}(x_i)|}{\max(\epsilon, |y_i|)}. \quad (5.1)$$

The performance of the algorithms is displayed in Figure 1. It can be observed that IGND and Adam have almost identical learning curves with Adam showing slightly faster convergence on the Diamonds dataset. Both methods significantly outperform SGD. While performing similarly, IGND has less per-iteration computational burden than Adam. The fastest convergence is, however, obtained by combining Adam with the scaling operation prescribed by IGND.

Algorithm 4 Gauss-Newton Policy Evaluation for LQR

- 1: **Input:** policy \mathbf{K} , initial weights \mathbf{w}_0 , learning rate α , discount factor γ , tolerance $\eta = 10^{-8}$, LM regularizer ϵ .
 - 2: Set policy evaluation counter $i = 1$
 - 3: Initialize S_1
 - 4: **repeat**
 - 5: Choose action $A_i \sim \pi(S_i)$ by following an exploratory policy $\pi(s) = \mathbf{K}s + e$
 - 6: Execute action A_i and observe R_i, S_{i+1}
 - 7: Obtain A' by following a greedy policy $\pi(s) = \mathbf{K}s$
 - 8: Convert $[S_i, A_i]$ and $[S_{i+1}, A']$ to quadratic feature vectors \mathbf{x} and \mathbf{x}'
 - 9: Calculate $\xi_i = 1/(\mathbf{x}^\top \mathbf{x} + \epsilon)$
 - 10: Calculate $\mathbf{d}_i = \xi_i [(R_i + \mathbf{w}_{i-1}^\top (\gamma \mathbf{x}' - \mathbf{x})) \mathbf{x}]$
 - 11: Update weights $\mathbf{w}_i \leftarrow \mathbf{w}_{i-1} + \alpha_i \mathbf{d}_i$
 - 12: Set $i = i + 1$
 - 13: **until** $\|\mathbf{w}_i - \mathbf{w}_{i-1}\|_\infty < \eta$
 - 14: **Return** \mathbf{w}_i
-

5.2 Tabular Reinforcement Learning

Tabular reinforcement learning is a form of RL in which the solution consists of a look-up table, i.e., each entry in the table represents the Q -value of a particular state and action pair (see a detailed overview in [39]). `FrozenLake-v1` is an example of such tabular reinforcement learning problems. It is an OpenAI Gym [5] environment structured as a 4-by-4 grid world with 4 actions and 16 states. The agent starts in the upper left corner with the goal to reach the bottom right state while at the same time avoiding “hole” cells. The agent receives a reward of 1 for reaching the goal state. The episode terminates in case a) the goal state is reached; or b) the agent steps into a hole; or c) the limit of 100 steps is reached.

As we discussed above, value-based RL algorithms, like Q-learning, can easily be IGND-adapted by multiplying the weight update by ξ . We call such variant of Q-learning IGNDQ.

The action-value function $q_{\mathbf{w}}(S_t, A_t)$ for tabular RL can be written as

$$q_{\mathbf{w}}(S_t, A_t) = \mathbf{w}_t^\top \mathbf{x}_t \tag{5.2}$$

with $\mathbf{x}_t = g(S_t, A_t)$ where the function $g(\cdot)$ creates a one-hot encoded (OHE) vector indicating the position in the look-up table, such that $\mathbf{x} \in \{0, 1\}^m$ and $\sum_{j=1}^m \mathbf{x}_j = 1$. We observe that only one weight is being updated per iteration, since

$$q_{\mathbf{w}}(S_t, A_t) = \mathbf{w}_t^\top \mathbf{x}_t = \mathbf{w}_t^{(j)} \mathbf{x}_t^{(j)} = \mathbf{w}_t^{(j)} \tag{5.3}$$

where j is the index of the non-zero feature \mathbf{x}_t corresponding to S_t, A_t . To illustrate the scale invariance property we multiply each feature by some fixed scalar $\phi^{(j)}$ resulting in

$$\tilde{q}_{\mathbf{w}}(S_t, A_t) = \phi^{(j)} \mathbf{w}_t^{(j)} \mathbf{x}_t^{(j)} = \phi^{(j)} \mathbf{w}_t^{(j)}. \tag{5.4}$$

For our experiments we pick a random integer uniformly from $[-10^4, 10^4]$ for each $\phi^{(j)}$. We run the simulations for both scaled and non-scaled features for 5000 steps with the best performing learning rate α after a grid search for $\alpha \in [10^{-9}, 1]$.

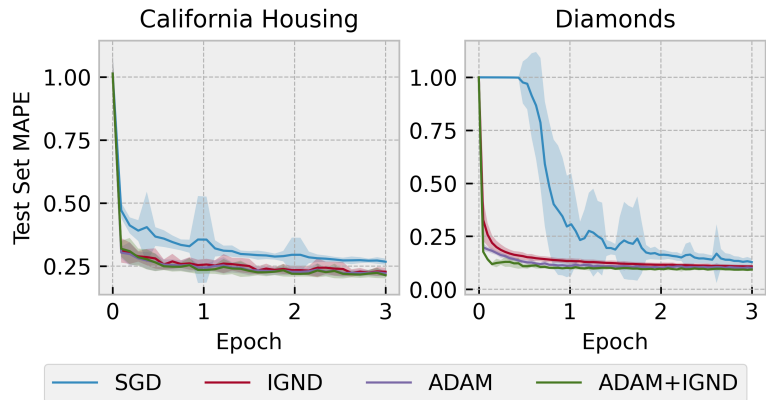


Figure 1: Learning curves on the test set for SGD, IGND, Adam and Adam applied on IGND-scaled gradients. The shaded area represents ± 1 standard deviation around the mean (thick line) for 20 seeds.

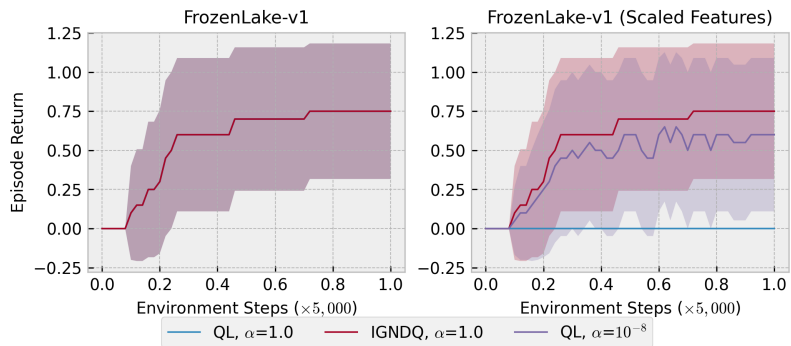


Figure 2: Learning curves for QL and IGNDQ on **FrozenLake-v1** environment with original (left plot) and scaled (right plot) features. The shaded area represents ± 1 standard deviation around the mean return (thick line) for 20 seeds.

The results of the experiments are presented in Figure 2. The learning curves for QL and IGNDQ are the same for the original (non-scaled) features, which is not surprising since $\nabla q_{\mathbf{w}} = 1$ implying $\xi = 1$. However, if we scale the features by ϕ , we notice that the IGNDQ learning curve is unaffected by scaling (confirming the scale invariance property of IGND presented in Section 3.5) while QL updates are completely compromised by scaling, requiring a new hyper-parameter search for a more suitable value of α (which in this case is $\alpha = 10^{-8}$).

5.3 RL with Function Approximation

We compare the performance of IGNDQ against the standard Q-learning (QL) algorithm [39] on two non-linear RL tasks with discrete action spaces – **Acrobot-v1** and **CartPole-v1**. **Acrobot-v1** is an OpenAI gym [5] environment where the goal is to swing the free end of the connected joints above a given height in as few steps as possible. **CartPole-v1** is another environment from the OpenAI gym where the goal is to balance a pole on a cart for as long as possible. For both environments, the function approximator $f_{\mathbf{w}}$ for the Q-network is an FFNN with 3 hidden layers having 32, 64 and 32 units, followed

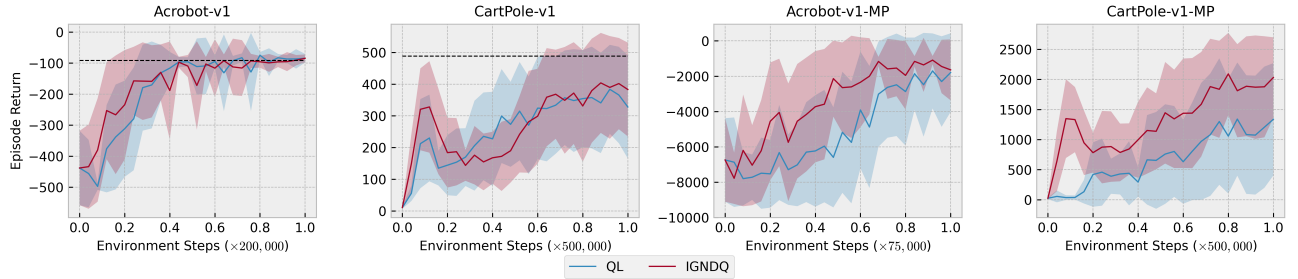


Figure 3: Learning curves for QL and IGNDQ on original **Acrobot-v1** and **CartPole-v1** and modified environments. The shaded area represents ± 1 standard deviation around the mean return (thick line) for 20 seeds. In the left plots, the black dashed line shows the performance of the CleanRL DQN trained agent.

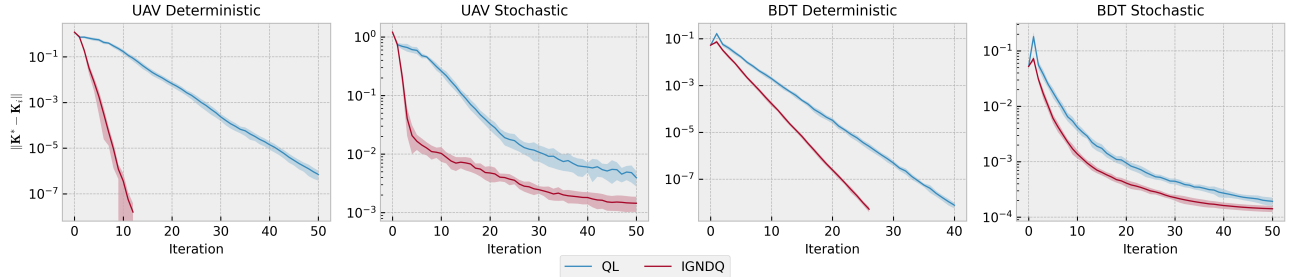


Figure 4: QL and IGNDQ learning curves against the optimal LQR controller for the deterministic and stochastic LQR formulations. The shaded area represents ± 1 standard deviation around the mean (thick line) return for 20 seeds.

by ReLU activation functions. We select the best performing learning rate α after a grid search for $\alpha \in [10^{-8}, 1]$. For reference we also provide the performance of the pre-trained DQN agent from the open-source baselines of CleanRL [16]. The results are shown in the left part of Figure 3, where it can be seen that by adequately selecting the learning rate α one can obtain comparable performance for IGNDQ and QL, and both converge to the pre-trained performance for **Acrobot-v1**, while they only approach it for **CartPole-v1**.

In order to highlight the benefits of IGNDQ, we also test the same environments with modified rewards. We introduce **Acrobot-v1-MP** where the reward is minus the square distance of the free end of the chain from the upwards position, such that

$$R_t = - \left(2 + \cos(S_t^{(1)}) + \cos(S_t^{(1)} + S_t^{(2)}) \right)^2 - \mathbb{I}[A_t \in \{1, 3\}], \quad (5.5)$$

where $S_t^{(1)}$ is the first component of the state vector (angle of the first joint), $S_t^{(2)}$ is the second component of the state vector (angle of the second joint relative to the angle of the first link) and $\mathbb{I}[A_t \in \{1, 3\}]$ is an indicator function that is equal to 1 if the torque is applied to the actuated joint and 0 otherwise. The intuition is that the closer the system is to the terminal state, the larger the reward is received, with additional penalty applied to a non-zero torque action. The modified **CartPole-v1-MP** reward is

minus the square of the angular difference between the current and the upward position,

$$R_t = \max \left\{ 5 - 100 \left(S_t^{(3)} \right)^2 - \left(S_t^{(4)} \right)^2, 0 \right\}, \quad (5.6)$$

where $S_t^{(3)}$ is the third component of the state vector (angle of the pole) and $S_t^{(4)}$ is the fourth component of the state vector (pole angular velocity).

The rationale behind modifying the original rewards is to introduce state dependency. The original reward is $[-1, 0]$ for **Acrobot-v1** and $[0, 1]$ for **CartPole-v1** regardless of which state the agent is in. In contrast, the modified reward is proportional to the proximity to the terminal state and takes values in the ranges $[-17, 0]$ and $[0, 5]$ for **Acrobot-v1-MP** and **CartPole-v1-MP** respectively. In that case, the use of IGND is especially beneficial for the reason of the scale-invariance property discussed in Section 3.5.

The results are displayed in the right plots of Figure 3, where it can be seen that even after tuning the learning rate α , QL performs worse than IGNDQ for both environments.

The hyperparameters for the Q-learning (QL) and Gauss-Newton Q-learning (IGNDQ) of **Acrobot-v1** and **CartPole-v1** experiments are presented in Table 1 and Table 2 respectively.

Table 1: Hyperparameters for **Acrobot-v1**

Parameter	QL	IGNDQ
Network architecture	[32,64,32]	[32,64,32]
Activation	ReLU	ReLU
Discount Factor γ	0.99	0.99
Exploration Fraction	1.0	1.0
Start ϵ	1.0	1.0
End ϵ	0.05	0.05
Target network update frequency	100	100
Learning rate α	0.0001	0.3

5.4 Linear Quadratic Regulator

IGNDQ can also be extended to RL problems with continuous action spaces. We modify the policy iteration procedure for Linear Quadratic Regulator (LQR) presented in [4] by multiplying the weight update by ξ (all details are provided in Section 4.2). We select two linear systems from the Compeib set of benchmarks [21]. The first system is the linearized vertical plane dynamics of an aircraft (UAV) [17] and the second one represents the model of a binary distillation tower (BDT) [8]. Both systems are discretized with a sampling rate of $\Delta T = 0.1s$. The reward function matrices are negative identity $\mathbf{Q} = -\mathbf{I}_{n_s}$, $\mathbf{R} = -\mathbf{I}_{n_a}$.

The results are displayed in Figure 4, where the performance of IGNDQ and QL is compared in terms of how well the policy matrix \mathbf{K} matches the optimal one \mathbf{K}^* . In this example, the difference between IGNDQ and QL is remarkable. This result is likely to have a strong impact on recently suggested applications of RL in automation [47, 48], where more elaborate controllers have a similar structure as the LQR, but are able to provide strong guarantees in terms of safety and stability.

The hyperparameters for the UAV and BDT experiments are presented in Table 3. and Table 4 respectively.

Table 2: Hyperparameters for CartPole-v1

Parameter	QL	IGNDQ
Network architecture	[32, 64, 32]	[32, 64, 32]
Activation	ReLU	ReLU
Discount Factor γ	0.99	0.99
Exploration Fraction	1.0	1.0
Start ϵ	1.0	1.0
End ϵ	0.05	0.05
Target network update frequency	100	100
Learning rate α	0.0001	0.1

Table 3: Hyperparameters for UAV

Parameter	QL	IGNDQ
Policy Evaluation Steps	1000	1000
Policy Improvement Steps	50	50
Initial Policy \mathbf{K}_0	$\mathbf{1} \times -0.01$	$\mathbf{1} \times -0.01$
Discount Factor γ	0.9	0.9
System Noise σ^2	0.01	0.01
Start Learning rate α	6×10^{-7}	1.0
End Learning rate α	1×10^{-8}	0.001

5.5 Impact of Hyperparameters

In line with [1] and [12], we observe that Gauss-Newton based methods require much less tuning than SGD. During the experiments we noticed that the optimal learning rate for SGD takes values ranging from 10^{-2} to 10^{-8} and even small deviations from the optimal learning rate can severely compromise convergence. For IGND we obtained good results for all the examples by picking $\alpha \in [1.0, 0.01]$. Additionally, even if a suboptimal learning rate was selected, convergence was not jeopardized, albeit the convergence was slower.

6 Conclusions and Future Work

We presented a Gauss-Newton incremental algorithm for ML and we demonstrated its effectiveness both in supervised learning and reinforcement learning problems. Our algorithm has a negligible overhead compared to standard SGD, but delivers more reliable convergence at a rate that is no smaller than the one of SGD; moreover, it can also be combined with any of the existing accelerated methods.

Future work will focus on generalized GN and its application to non least-squares loss functions, which are relevant in many machine learning applications. Further research will also be devoted to studying in depth the effect of IGND on RL algorithms, e.g., by combining it with variations of Q-learning, as proposed in [13]. Finally, our method can be extended to batch algorithms while retaining a reasonably small computational complexity, which is the subject of ongoing research.

Table 4: Hyperparameters for BDT

Parameter	QL	IGNDQ
Policy Evaluation Steps	1000	1000
Policy Improvement Steps	50	50
Initial Policy \mathbf{K}_0	$\mathbf{1} \times -0.01$	$\mathbf{1} \times -0.01$
Discount Factor γ	0.9	0.9
System Noise σ^2	0.001	0.001
Start Learning rate α	1×10^{-7}	1.0
End Learning rate α	1×10^{-8}	0.001

References

- [1] Aleksandar Botev, Hippolyt Ritter, and David Barber. Practical Gauss-Newton optimisation for deep learning. In *International Conference on Machine Learning*, pages 557–565. PMLR, 2017. (Cited on pages 3 and 23.)
- [2] Léon Bottou, Frank E Curtis, and Jorge Nocedal. Optimization methods for large-scale machine learning. *SIAM review*, 60(2):223–311, 2018. (Cited on pages 3, 11, 12, and 13.)
- [3] Léon Bottou et al. Online learning and stochastic approximations. *On-line learning in neural networks*, 17(9):142, 1998. (Cited on page 13.)
- [4] Steven J Bradtke, B Erik Ydstie, and Andrew G Barto. Adaptive linear quadratic control using policy iteration. In *Proceedings of 1994 American Control Conference-ACC'94*, volume 3, pages 3475–3479. IEEE, 1994. (Cited on pages 17 and 22.)
- [5] Greg Brockman, Vicki Cheung, Ludwig Pettersson, Jonas Schneider, John Schulman, Jie Tang, and Wojciech Zaremba. OpenAI Gym, 2016. (Cited on pages 19 and 20.)
- [6] Johannes J Brust. Nonlinear least squares for large-scale machine learning using stochastic Jacobian estimates. *arXiv preprint arXiv:2107.05598*, 2021. (Cited on pages 2 and 3.)
- [7] John Chen, Cameron Wolfe, Zhao Li, and Anastasios Kyrillidis. Demon: improved neural network training with momentum decay. In *ICASSP 2022-2022 IEEE International Conference on Acoustics, Speech and Signal Processing (ICASSP)*, pages 3958–3962. IEEE, 2022. (Cited on pages 1 and 3.)
- [8] Edward J Davison. Benchmark problems for control system design. *Report of the IFAC Theory Committee*, 1990. (Cited on page 22.)
- [9] Timothy Dozat. Incorporating Nesterov momentum into Adam. 2016. (Cited on pages 1 and 3.)
- [10] John Duchi, Elad Hazan, and Yoram Singer. Adaptive subgradient methods for online learning and stochastic optimization. *Journal of machine learning research*, 12(7), 2011. (Cited on pages 1 and 3.)

- [11] Vincent François-Lavet, Peter Henderson, Riashat Islam, Marc G Bellemare, Joelle Pineau, et al. An introduction to deep reinforcement learning. *Foundations and Trends® in Machine Learning*, 11(3-4):219–354, 2018. (Cited on page 16.)
- [12] Matilde Gargiani, Andrea Zanelli, Moritz Diehl, and Frank Hutter. On the promise of the stochastic generalized Gauss-Newton method for training DNNs. *arXiv preprint arXiv:2006.02409*, 2020. (Cited on pages 2, 3, 6, and 23.)
- [13] Matteo Hessel, Joseph Modayil, Hado Van Hasselt, Tom Schaul, Georg Ostrovski, Will Dabney, Dan Horgan, Bilal Piot, Mohammad Azar, and David Silver. Rainbow: Combining improvements in deep reinforcement learning. In *Thirty-second AAAI conference on artificial intelligence*, 2018. (Cited on page 23.)
- [14] Geoffrey Hinton, Nitish Srivastava, and Kevin Swersky. Neural networks for machine learning. Lecture 6a overview of mini-batch gradient descent. *Cited on*, 14(8):2, 2012. (Cited on pages 1 and 3.)
- [15] Yuxi Hong, Houcine Bergou, Nicolas Doucet, Hao Zhang, Jesse Cranney, Hatem Ltaief, Damien Gratadour, Francois Rigaut, and David E Keyes. Stochastic Levenberg-Marquardt for solving optimization problems on hardware accelerators. Submitted to IEEE, 2020. (Cited on page 3.)
- [16] Shengyi Huang, Rousslan Fernand Julien Dossa, Chang Ye, and Jeff Braga. Cleanrl: High-quality single-file implementations of deep reinforcement learning algorithms. *arXiv preprint arXiv:2111.08819*, 2021. (Cited on page 21.)
- [17] YS Hung and AGJ MacFarlane. Multivariable control: A quasiclassical approach, 1982. (Cited on page 22.)
- [18] Diederik P Kingma and Jimmy Ba. Adam: A method for stochastic optimization. *arXiv preprint arXiv:1412.6980*, 2014. (Cited on pages 1 and 3.)
- [19] Ryan Kiros. Training neural networks with stochastic Hessian-free optimization. *arXiv preprint arXiv:1301.3641*, 2013. (Cited on page 3.)
- [20] Guanghai Lan. *First-order and stochastic optimization methods for machine learning*, volume 1. Springer, 2020. (Cited on page 2.)
- [21] F Leibfritz. Compleib: Constrained matrix optimization problem library, 2006. (Cited on page 22.)
- [22] Huan Li, Cong Fang, and Zhouchen Lin. Accelerated first-order optimization algorithms for machine learning. *Proceedings of the IEEE*, 108(11):2067–2082, 2020. (Cited on pages 1 and 2.)
- [23] James Lucas, Shengyang Sun, Richard Zemel, and Roger Grosse. Aggregated momentum: Stability through passive damping. *arXiv preprint arXiv:1804.00325*, 2018. (Cited on pages 1 and 2.)
- [24] James Martens et al. Deep learning via Hessian-free optimization. In *ICML*, volume 27, pages 735–742, 2010. (Cited on page 3.)
- [25] James Martens and Roger Grosse. Optimizing neural networks with kronecker-factored approximate curvature. In *International conference on machine learning*, pages 2408–2417. PMLR, 2015. (Cited on page 3.)

- [26] Kevin P. Murphy. *Probabilistic Machine Learning: An introduction*. MIT Press, 2022. (Cited on page 4.)
- [27] Ryan Murray, Brian Swenson, and Soumya Kar. Revisiting normalized gradient descent: Fast evasion of saddle points. *IEEE Transactions on Automatic Control*, 64(11):4818–4824, 2019. (Cited on pages 4 and 9.)
- [28] Mor Shpigel Nacson, Jason Lee, Suriya Gunasekar, Pedro Henrique Pamlona Savarese, Nathan Srebro, and Daniel Soudry. Convergence of gradient descent on separable data. In *The 22nd International Conference on Artificial Intelligence and Statistics*, pages 3420–3428. PMLR, 2019. (Cited on pages 4 and 9.)
- [29] Yurii Nesterov. A method of solving a convex programming problem with convergence rate $O(1/k^2)$. *Doklady Akademii Nauk SSSR*, 269(3):543, 1983. (Cited on pages 1 and 2.)
- [30] J. Nocedal and S. Wright. *Numerical Optimization*. Springer Series in Operations Research and Financial Engineering. Springer New York, 2006. (Cited on pages 2, 6, and 10.)
- [31] R Kelley Pace and Ronald Barry. Sparse spatial autoregressions. *Statistics & Probability Letters*, 33(3):291–297, 1997. (Cited on page 18.)
- [32] Boris T Polyak. Some methods of speeding up the convergence of iteration methods. *Ussr computational mathematics and mathematical physics*, 4(5):1–17, 1964. (Cited on page 2.)
- [33] Jiang Qian, Yuren Wu, Bojin Zhuang, Shaojun Wang, and Jing Xiao. Understanding gradient clipping in incremental gradient methods. In *International Conference on Artificial Intelligence and Statistics*, pages 1504–1512. PMLR, 2021. (Cited on page 4.)
- [34] Yi Ren and Donald Goldfarb. Efficient subsampled gauss-newton and natural gradient methods for training neural networks. *arXiv preprint arXiv:1906.02353*, 2019. (Cited on pages 2 and 3.)
- [35] Herbert Robbins and Sutton Monro. A stochastic approximation method. *The annals of mathematical statistics*, pages 400–407, 1951. (Cited on pages 1, 2, 5, and 13.)
- [36] Levent Sagun, Utku Evci, V Ugur Guney, Yann Dauphin, and Leon Bottou. Empirical analysis of the hessian of over-parametrized neural networks. *arXiv preprint arXiv:1706.04454*, 2017. (Cited on page 5.)
- [37] Shiliang Sun, Zehui Cao, Han Zhu, and Jing Zhao. A survey of optimization methods from a machine learning perspective. *IEEE transactions on cybernetics*, 50(8):3668–3681, 2019. (Cited on page 2.)
- [38] Ilya Sutskever, James Martens, George Dahl, and Geoffrey Hinton. On the importance of initialization and momentum in deep learning. In *International conference on machine learning*, pages 1139–1147. PMLR, 2013. (Cited on pages 1 and 2.)
- [39] Richard S Sutton and Andrew G Barto. *Reinforcement learning: An introduction*. MIT press, 2018. (Cited on pages 16, 19, and 20.)

- [40] Quoc Tran-Dinh, Nhan Pham, and Lam Nguyen. Stochastic Gauss-Newton algorithms for nonconvex compositional optimization. In *International Conference on Machine Learning*, pages 9572–9582. PMLR, 2020. (Cited on pages 2 and 3.)
- [41] Oriol Vinyals and Daniel Povey. Krylov subspace descent for deep learning. In *Artificial intelligence and statistics*, pages 1261–1268. PMLR, 2012. (Cited on page 3.)
- [42] Haozhao Wang, Zhihao Qu, Qihua Zhou, Haobo Zhang, Boyuan Luo, Wenchao Xu, Song Guo, and Ruixuan Li. A comprehensive survey on training acceleration for large machine learning models in iots. *IEEE Internet of Things Journal*, 2021. (Cited on page 1.)
- [43] Hadley Wickham. *ggplot2: Elegant Graphics for Data Analysis*. Springer-Verlag New York, 2016. (Cited on page 18.)
- [44] Bernard Widrow and Samuel D Stearns. Adaptive signal processing prentice-hall. *Englewood Cliffs, NJ*, 1985. (Cited on page 4.)
- [45] Peng Xu, Fred Roosta, and Michael W Mahoney. Second-order optimization for non-convex machine learning: An empirical study. In *Proceedings of the 2020 SIAM International Conference on Data Mining*, pages 199–207. SIAM, 2020. (Cited on pages 1 and 3.)
- [46] Manzil Zaheer, Sashank Reddi, Devendra Sachan, Satyen Kale, and Sanjiv Kumar. Adaptive methods for nonconvex optimization. *Advances in neural information processing systems*, 31, 2018. (Cited on page 1.)
- [47] M. Zanon and S. Gros. Safe Reinforcement Learning Using Robust MPC. *IEEE Transactions on Automatic Control*, 66(8):3638–3652, 2021. (Cited on page 22.)
- [48] M. Zanon, S. Gros, and M. Palladino. Stability-Constrained Markov Decision Processes Using MPC. *Automatica*, 2022. (in press). (Cited on page 22.)
- [49] Matthew D Zeiler. Adadelta: an adaptive learning rate method. *arXiv preprint arXiv:1212.5701*, 2012. (Cited on pages 1 and 3.)
- [50] Jingzhao Zhang, Tianxing He, Suvrit Sra, and Ali Jadbabaie. Why gradient clipping accelerates training: A theoretical justification for adaptivity. *arXiv preprint arXiv:1905.11881*, 2019. (Cited on pages 4 and 9.)